Biosensors and Bioelectronics 28 (2011) 320–325

Contents lists available at ScienceDirect

Biosensors and Bioelectronics

journal homepage: www.elsevier.com/locate/bios

P450-based porous silicon biosensor for arachidonic acid detection

A.M. Giovannozzi[a,*,1], V.E.V. Ferrero[c,1], F. Pennecchi[b], S.J. Sadeghi[c], G. Gilardi[c], A.M. Rossi[a]

[a] Thermodynamic Division, Istituto Nazionale di Ricerca Metrologica, Strada delle Cacce 91, 10135 Torino, Italy
[b] Mechanical Division, Istituto Nazionale di Ricerca Metrologica, Strada delle Cacce 91, 10135 Torino, Italy
[c] Centre of Excellence in Nanostructured Interfaces and Surfaces – Department of Human and Animal Biology, University of Torino, Via Accademia Albertina 13, 10123 Torino, Italy

ARTICLE INFO

Article history:
Received 27 June 2011
Accepted 17 July 2011
Available online 22 July 2011

Keywords:
Porous silicon
Biosensor
Fluorescence
Arachidonic acid
P450 BM3

ABSTRACT

A porous silicon biosensor based on P450 enzyme for arachidonic acid detection was developed. A new transduction method is presented with a simultaneous measurement of refractive index and fluorescence intensity changes when the analyte is binding to an enzyme on the porous silicon surface. A fluorophore bound to a cysteine residue in an allosteric position of the haem domain (BMP) of cytochrome P450 BM3 enhances its fluorescence intensity upon interaction with its substrate arachidonic acid, involved in diseases such as Alzheimer's, liver cancer and cellular inflammation processes. BMP has been anchored on porous silicon surface and the new transduction method has been successfully exploited to develop a biosensor for arachidonic acid, reaching a detection limit of 10 μM arachidonic acid in a dynamic range of 10–200 μM. Moreover, the change of the refractive index has been also monitored at the same time, displaying a higher detection limit of 30 μM. Preliminary test were also conducted in plasma proving the high specificity and selectivity of the sensor even in presence of interferents in the range of 50–100 μM. Here we suggest these two detection systems could be used simultaneously to increase the accuracy and the dynamic range of the sensor avoiding a false positive response.

1. Introduction

Immobilization of biomolecules on solid supports has received great interest in emerging technologies to develop systems based on biocatalytic and biorecognition events (DeLouise and Miller, 2005). These technologies include the development of biosensors for several class of analytes such as pathogens (Chan et al., 2001a,b), toxins (Ligler et al., 2003), tumoral markers (Wang, 2006), drugs; micro- and nano-array for genomic and proteomic analysis (MacBeath, 2001; Fantuzzi et al., 2010; Panico et al., 2011; Sadeghi et al., 2011); and enzymes for bioreactors (Davison and Nghiem, 1999).

For biosensing applications, nanoscale materials with their large, often highly reactive surface, and their ability of interacting with biomolecules of comparable dimension, can provide a more effective capture and detection of molecules when compared to bulk materials (Rossi et al., 2007). One such material, nanoporous silicon, has been widely studied in the last two decades as an optical transducer for biosensors, due to its intrinsic properties and to the easy and cheap fabrication processes (Canham, 1997). The high specific surface area (200 m^2/cm^3) and the possibility to anchor biomolecules as capture probes give high sensibility and specificity of interaction to a defined target. Moreover, the high optical quality of porous silicon (PS) layers allows the realization of label free optical devices from a simple monolayer (Lin et al., 1997) to more complex structures such as Fabry-Perot microcavity (Chan et al., 2001a,b; De Stefano et al., 2004), Bragg reflectors (Snow et al., 1999), rugate filters (Pacholski et al., 2006) and waveguide (Rong et al., 2008). However, the optical signal generated by a change of the refractive index of the porous layer upon the infiltration of the biomolecule provides only an incomplete picture of the device and could allow for false positives due to the infiltration of several molecules within a complex solution.

In order to achieve a more specific response of the enzyme-substrate interaction, we present an alternative and fast transduction method based on the fluorescence changes of a fluorophore labeled engineered enzyme. Labeling of specific cysteine residues close to the binding site of several periplasmic binding proteins for studying ligand binding has been previously exploited by our group as well as others (Gilardi et al., 1994; De Lorimier et al., 2002), together with antibodies (Renard and Bedouelle, 2004) and enzymes (Der and Dattelbaum, 2008).

Cytochrome P450 BM3 (CYP102A1) from *Bacillus megaterium* is a catalytically self-sufficient monooxygenase. It is composed of a haem domain (BMP) fused via a peptide linker to the reductase domain in a single polypeptide chain of 119 kDa (Narhi and Fulco, 1986). Recently, our group has generated a cysteine mutant of BMP that was labeled with a fluorophore that senses the binding of its substrate arachidonic acid (AA) to its active site. Conforma-

* Corresponding author. Tel.: +39 011 3919325; fax: +39 011 346384.
E-mail address: a.giovannozzi@inrim.it (A.M. Giovannozzi).
[1] These authors have contributed equally to this work.

0956-5663/$ – see front matter © 2011 Elsevier B.V. All rights reserved.
doi:10.1016/j.bios.2011.07.046

tional rearrangements in BMP upon binding of the substrate lead to changes in the environment of the fluorophore and hence to an enhancement of the fluorescent emission that is proportional to the concentration of AA (Ferrero et al., 2011).

Since AA is a well known biomarker involved in pain and inflammation processes (Hain, 1997; Serhan et al., 2004; Wyss-Coray and Mucke, 2002; Dai et al., 2001; Roman, 2002; Panigrahy et al., 2010), in neuronal development (Darios and Davletov, 2006) and also in a number of diseases such as Alzheimer's (Sanchez-Mejia and Mucke, 2010), liver cancer (Dymkowska and Wojtczak, 2009; Panigrahy et al., 2010; Xu et al., 2010), kidney pathologies (Kauser et al., 1991; Su et al., 1998) and blood pressure dysregulation (Nguyen et al., 1999; Zeldin et al., 1996) we decided to develop a biosensing platform based on PS for its detection. In this work, an AA biosensor has been developed through the immobilization of the fluorophore-labeled BMP in PS exploiting two different transduction methods at the same time. The first is based on the fluorescence variation of the fluorophore-labeled BMP, the other on the change in refractive index. Both methods have been successfully employed and combined to increase the dynamic range of the sensor and to avoid false positive responses.

2. Materials and methods

2.1. Protein expression and purification

The protein was expressed, isolated and purified (Ferrero et al., 2008) and functionality of purified BMP enzymes was verified spectrophotometrically (Omura and Sato, 1964).

2.2. Protein labeling

The active and pure protein (purity ratio $Abs_{419}/Abs_{280} = 1.3$) was pre-incubated with a fivefolds excess of dithiothreitol (DTT) for 30 min at 4 °C to reduce intermolecular disulphide bonds. After removing the excess DTT with a PD10 Sephadex G25 column (GE Healthcare), the fluorescent probe IANBD amide (absorption λ_{max} 478 nm, emission λ_{max} 540 nm) in a tenfolds excess was added to the protein solution and the mixture was incubated for 3 h at 4 °C. The protein reacts with the probe through its thiol group, forming a thioether bond.

The excess probe was then removed by a PD10 Sephadex G25 column. The Cf/Cp ratio (Ferrero et al., 2011), that indicates the labeling ratio obtained for the protein, was measured spectrophotometrically (UV–vis spectrophotometer Agilent 8453E, Agilent Technologies).

2.3. Porous film preparation

The PS films were prepared using pulsed anodic etching in an HF electrolyte solution (Foll, 1991). A homemade PVC electrochemical cell was equipped with a platinum sheet as a cathode and a polished p^+-doped crystalline silicon wafer as the anode (⟨1 0 0⟩ boron doped, $\rho = 8–12\ m\Omega\ cm$, MEMC). Etching was performed using a sequence of current pulses (200 ms pulse duration followed by a 10 s pause), supplied by a programmable current generator (Keithley 2400). A sacrificial layer was first prepared using a 1:1 hydrofluoric acid (50% in water) ethyl alcohol (>99.9%) solution and applying a current density of 300 mA/cm^2 for a total etching time of 1 s and subsequently dissolved in 1 M KOH aqueous solution. The PS layer has been fabricated etching the prestructured silicon wafer with a 1: 2.3 hydrofluoric acid (50% in water) ethyl alcohol (>99.9%) solution and applying a current density of 70 mA/cm^2. PS layers were etched to a depth of 2.5 or 5 μm. The thickness of the PS samples was measured using a Tencor P-100 profilometer after dissolution in 1 M KOH aqueous solution. After forming the porous layers, the chips were rinsed in deionized water and ethanol and subsequently dried with N_2 gas.

2.4. SEM characterization

Sample characterization was carried out using scanning electron microscopy (SEM) FEI Quanta 3D or Inspect F in UHV mode with the SE detector. Typical settings for the imaging are: 30 kV accelerating voltage, 1.5 spot (17 pA with 30 μm aperture), 10 mm WD.

2.5. Bioconjugation chemistry

Freshly etched PS samples were partially thermally oxidized in a furnace at 500 °C for 3 h in an air atmosphere and subsequently exposed to a 1 M aqueous NaOH for 2 min. This was followed by treating the samples with a 5% solution of (3-aminopropyl)-trimethoxysilane (APTMS) (>95% from Sigma–Aldrich) in ethanol (>99.9% from Carlo Erba) mixing for 4 h at room temperature. Samples were gently rinsed with ethanol, dried gently with nitrogen and cured at 150 °C overnight (Vrancken et al., 1995). The silanized samples were then immersed in a 2.5% solution of glutaraldehyde in DI water (pH adjusted to 7 with NaOH) for 1 h at room temperature. Samples were extensively rinsed with DI water, immersed in deionized water for 10 min twice and dried with nitrogen flux. IANBD labeled BMP (2, 5 and 10 μM) in phosphate buffer solution (KPi 100 mM, pH 7.4) has been dropped on glutaraldehyde activated surfaces and allowed to react for 2 h at room temperature. Several washing procedures have been used after the bioconjugation to remove the unreacted and absorbed proteins: porous silicon samples have been rinsed and incubated in KPi buffer pH 7.4 for 20 min, then rinsed and incubated in deionized water for 10 min twice. Finally, samples were dried with nitrogen and prepared for fluorescence and reflectivity measurements. For arachidonic acid incubation experiments, a 16.4 mM stock solution of AA in ethanol was first diluted to 1.64 mM in K_2CO_3 and further diluted to the desired concentrations of 200, 150, 100, 80, 50, 30 and 10 μM in phosphate buffer solution (KPi). PS samples were incubated in AA solutions for 30 min, then extensively rinsed and soaked in KPi for 5 min, then in deionized water for the same time and finally dried with nitrogen.

For the analysis on a real matrix, human blood (5 ml) was drawn from vein and collected in a tube containing EDTA. The erythrocytes were then separated by centrifugation (3000 rpm for 10 min) and the supernatant plasma collected and used for further analysis. Plasma was used as is or with additions of different amounts of arachidonic acid (50, 100 and 200 μM). PS samples with the labeled BMP were then incubated with these solutions as previously described.

2.6. FTIR characterization

The infrared spectra of PS samples were collected using Nicolet Nexus equipped with Nicolet Continuum FTIR Microscope operating in reflectance mode; 64 interferograms, with a resolution of 4 cm^{-1}, were registered for each spectrum. Background spectrum was collected on c-Si after dipping in 25% HF to remove the native oxide.

2.7. Fluorescence and reflectivity analysis

The amount of IANBD labeled protein bound to the PS surface was quantified by measuring the dye-labeled fluorescence intensity at the emission peak (540 nm). The emission spectra were recorded using a fluorescence microscope equipped with a 20× objective and an external fiber optic mounted at the top of the microscope. The emitted light from PS samples was collected by

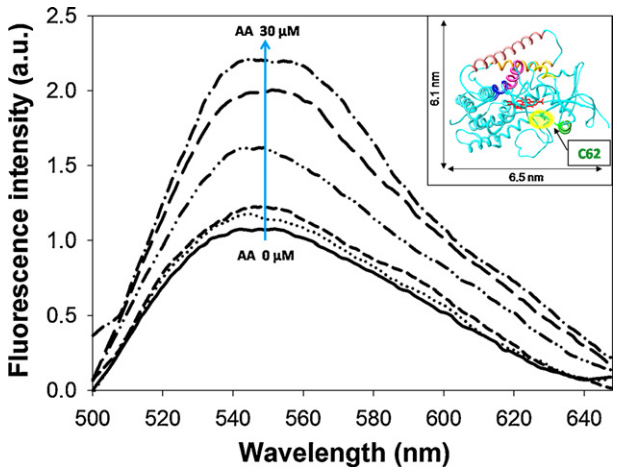

Fig. 1. Fluorescence emission spectra of 1 µM BMPwt IANBD-bound collected upon addition of increasing concentrations of AA from 0 to 30 µM. Inset: crystallographic 3D structure of BMP (PDB file 1FAG) showing the solvent exposed Cys62 (green, exposure of 11.0 Å^2) that was exploited as the linking site for the fluorescent probe (IANBD amide, yellow) on the protein. Some of the helices involved in changes upon substrate binding are coloured: helix B is green, B′ is yellow, F is orange, G is pink, H is magenta and I is blue. (For interpretation of the references to color in this figure legend, the reader is referred to the web version of the article.)

the optical fiber in back scattering configuration and transmitted to the detector (USB 2000 Fiber Optic Spectrometer, Ocean Optics). Metal halide lamp filtered with an emission peak at 488 nm was used as excitation source. Five measurements on PS surface were done for each sample using an integration time of 0.5 s. Reflectivity spectra were recorded with the same setup of fluorescence measurements using a white light lamp and a 10× microscope objective. Background spectrum was collected on a gold slide and automatically subtracted by the software from PS spectra. Three spectra on porous region were collected for each sample.

3. Results

Samples of pure protein with a purity index greater than 1.3 (Li et al., 1991) were labeled with a fluorescent probe (IANBD amide) that is able to covalently bind to thiol groups, exploiting a solvent exposed cysteine, the C62 (inset of Fig. 1). This residue is located in a loop between B and B′ helices close to the active site of the enzyme (Peterson and Graham, 1998). When the binding of AA occurs, there is a big movement of helices F and G (called lid part of the protein) that subsequently extends to helices H and I. Moreover, the B′ helix, which is in contact with the G helix, also moves with the lid domain (Haines et al., 2001). When the fluorophore is conjugated to the protein through the C62, it is be able to sense the microenvironment changes upon ligand binding, causing a variation in the fluorescence intensity.

BMP ligand binding studies were carried out using a range of AA concentrations from 0 to 30 µM: titrations of fluorophore-labeled BMP wild type resulted in a progressive enhancement of the probe fluorescence emission (λ_{em} = 540 nm) as shown in Fig. 1 (Ferrero et al., 2011).

The ability of the probe to increase its fluorescence intensity upon ligand binding was then tested when the wild type protein was immobilized on a surface, in order to create a biosensing platform initially for AA detection but subsequently for screening of other substrates.

PS monolayers with thickness ranging from 2.5 to 5 µm were fabricated to develop and optimize the AA biosensor. The PS fabrication protocol was adjusted to tune the pore dimensions to the biomolecule size (inset of Fig. 1).

Top view and cross section images of these PS samples are shown in Fig. 2. Pore size distribution analysis performed on PS top view image revealed an average pore size of 50 nm (Fig. 2a).

These pore dimensions guaranteed a higher BMP infiltration than those observed with mesoporous (ø 20 nm) and macroporous (ø 100 nm) silicon (data not shown). In the mesoporous case, pore dimensions are probably too small to induce a complete infiltration of the BMP inside the porous layer. In the case of macroporous silicon, the specific surface area is probably reduced, decreasing the amount of BMP anchored on the surface and affecting the sensitivity of the sensor. Thus, PS monolayers with 50 nm pores diameter were used to develop the sensor. Freshly etched hydride-terminated PS samples were thermally oxidized in a furnace at 500 °C for 3 h in order to form a silicon oxide layer at the internal and external surface of the porous film. In Fig. 3a FTIR spectra of PS layer with 4 µm thickness before and after the oxidation procedure are presented.

Typical absorption bands corresponding to stretching and deformation vibrations of SiH_x, $\nu(SiH_x)$ around 2100 cm^{-1} and $\delta(SiH_2)$ around 900 cm^{-1}, are shown in the "as-etched" spectrum. After the thermal oxidation, these bands disappear and the oxidized spectrum exhibits a large band centered at 1100 cm^{-1}, corresponding to stretching vibrations of $Si–O_x$ groups. Samples were then exposed to a solution of 1 M aqueous NaOH in order to hydrolyze the surface siloxane groups formed during thermal oxidation treatment. In this way more surface silanol groups are generated making the further silanization reaction more efficient (Cunin et al., 2007). FTIR spectrum of the APTMS silanized surface (Fig. 3b) show two small bands at 3294 cm^{-1} and near 3380 cm^{-1}, which are attributed to –NH bonds. Two bands around 3000–2800 cm^{-1} are due to the presence of $–CH_x$ bonds.

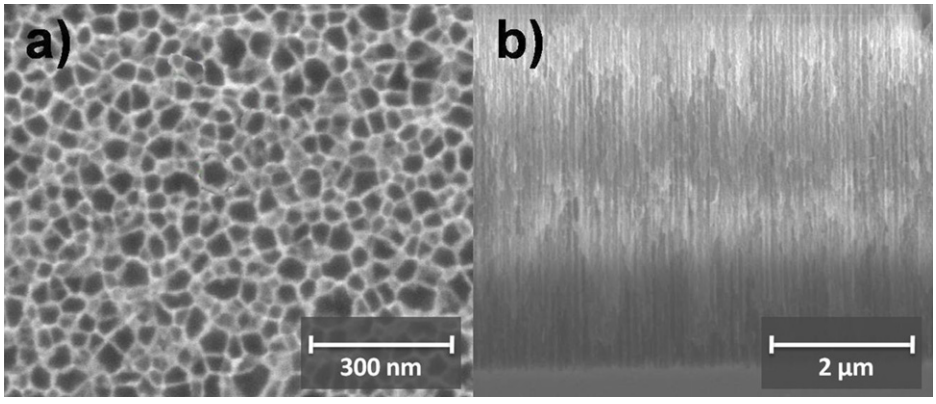

Fig. 2. (a) Top down and (b) cross sectional scanning electron micrographs of the PS films produced by electro-chemical etching.

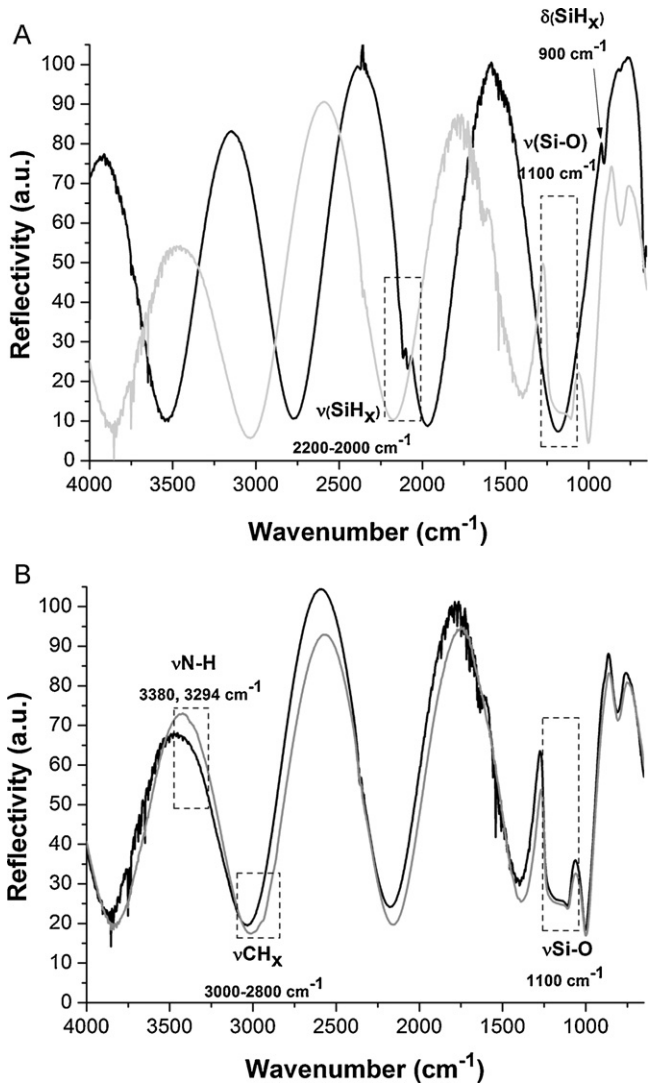

Fig. 3. (a) FTIR spectra of as-etched (black line) and thermally oxidized (grey line) PS; (b) FTIR spectra of thermally oxidized (black line) and APTMS silanized (grey line) PS.

The amine group of APTMS modified surface was reacted with glutaraldehyde to yield an aldehyde which can form an imine linkage with the primary amine group present in proteins.

Three concentrations (2, 5 and 10 μM) of IANBD-labeled BMP were grafted on PS monolayers and these samples were subsequently incubated with 200 μM of AA in order to validate the fluorescence transduction method and to identify the BMP concentration more sensitive to substrate addition. Accordingly to what we have seen in liquid measurements, upon the incubation with the arachidonic acid a fluorescence enhancement was detected on every PS samples while no fluorescence variation was seen in phosphate buffer solution (data not shown), suggesting the fluorescence change is only related to binding the BMP-AA. The highest fluorescence enhancement as well as a better sensitivity was reached when 10 μM of BMP was immobilized into the PS surface. After having positively tested the fluorescence transduction method and optimized the bioconjugation protocol, the dynamic range and the sensitivity of the sensor in buffer solution was investigated. PS samples bioconjugated with 10 μM of BMP were exposed to a series of solutions with AA concentrations ranging from 10 to 200 μM. Higher concentrations of AA were not tested due to a partial protein unfolding when AA above 200 μM was used in fluorescence titration measurements (data not shown). Moreover, in order to anchor a higher amount of BMP and to gain the sensitivity of the sensor, the thickness of the PS sample was increased up to 5 μm. In Fig. 4a the fluorescence change, calculated as the difference of the fluorescence intensity before and after the incubation with AA, is plotted against the AA concentration.

The fluorescence enhancement is linear up to 100 μM of AA with a good determination coefficient of 0.9952. As the AA concentration increases above 100 μM the sensor response is no longer linear and a saturation of the fluorescence seems to take over. A second order fit seems to suit perfectly in the dynamic range of 0–200 μM AA with a determination coefficient of 0.9955. From the data shown in Fig. 4a, a detection limit of 10 μM of AA was calculated.

Refractive index changes due to presence of AA inside the PS based on the shift of the interference fringe pattern in the visible range were also exploited as a parallel transduction method to combine two different transduction systems. In Fig. 4b the fringe pattern shift is plotted against the AA concentration. Differently from what we observed for the fluorescence transduction method, the sensor response based on the refractive index seems to be linear over the entire concentrations range of AA, as was confirmed by a determination coefficient of 0.9861 in the linear fit. However, the sensitivity of this method seems to be impaired at lower concentrations since 10 μM of AA is no longer detected. From the data shown in Fig. 4b, a detection limit of 30 μM of AA was calculated.

The sensor response both in fluorescence and refractive index measurements was also investigated in a complex matrix such as plasma in order to evaluate the specificity and the selectivity of these two transduction methods.

Three specific concentrations of AA (50, 100 and 200 μM) were added in plasma and subsequently incubated with the BMP modified porous silicon samples.

In Fig. 4c the fluorescence variation, calculated as the difference of the fluorescence intensity of PS samples exposed to plasma–AA solution and only plasma, is plotted against the AA concentration.

The fluorescence enhancement in a real sample seems to be linear over the concentration range of AA with a good determination coefficient of 0.9925.

A similar response was also obtained monitoring the refractive index changes upon incubation with AA (Fig. 4d). The shift of the interference fringe pattern of the samples incubated with plasma–AA solution has been subtracted to those incubated only with plasma and plotted versus the AA concentration.

Interestingly, a linear response was also obtained as confirmed by a determination coefficient of 0.9998.

4. Discussion

In the sensing test using AA standard buffer solutions the fluorescence method has shown to be more sensitive at lower concentrations of AA displaying a lower detection limit of 10 μM. From the data shown in Fig. 4a and b the fluorescence response seems to be linear up to 100 μM and tends to a saturation point above this value, while the refractive index method is linear all over the dynamic range of 10–200 μM. In the real sample analysis (Fig. 4c and d), instead, a linear response of both transduction methods was always observed.

Comparing the sensor response in standard buffer solutions and plasma for both fluorescence and refractive index measurements, some interesting information can be extracted (Fig. 4).

Comparing the fluorescence variation of the sensor upon the incubation of AA in plasma and buffer (only in the linear part of the fit in the range 0–100 μM AA), it is clearly seen that the slope of the line in buffer is slightly steeper than in plasma (Fig. 4a–c). The sensitivity of the fluorescence method in plasma, especially at low

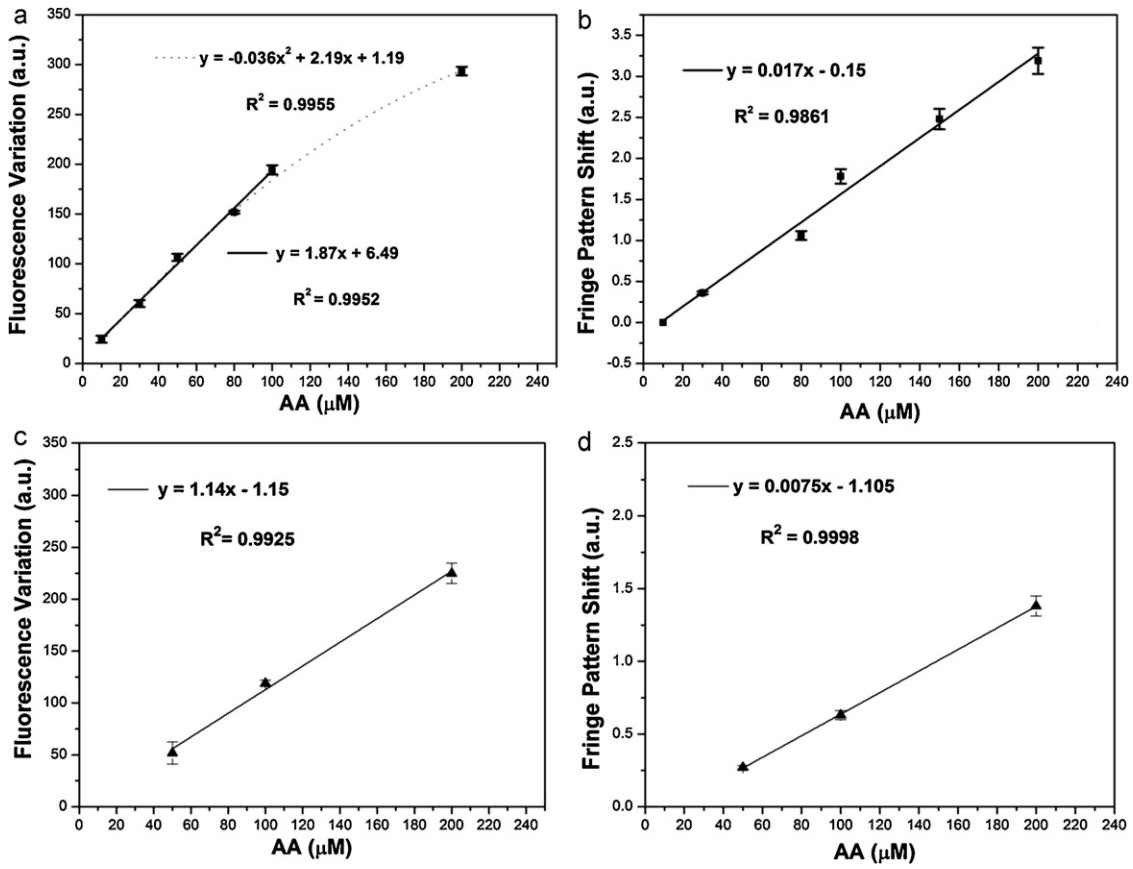

Fig. 4. (a) Fluorescence variation in KPI buffer is plotted over AA concentration. Linear fit in the 10–100 μM AA range (solid line) and parabolic fit in the 10–200 μM AA range (dotted line) are shown. (b) Fringe pattern shift in KPI buffer is plotted over the AA concentrations. Linear fit in the 10–200 μM AA range is shown. (c) Fluorescence variation in plasma is plotted over AA concentration. Linear fit in the 50–200 μM AA range is shown. (d) Fringe pattern shift in plasma is plotted over the AA concentrations. Linear fit in the 50–200 μM AA range is shown.

concentrations of AA, is barely affected by the presence of several interferents that can absorb the excitation/emission light. However, the fluorescence variation is still significantly detectable in the AA concentrations tested and a linear response was registered over the entire range.

The sensor response in the refractive index measurements (Fig. 4b–d) resulted to be linear over the entire range tested. However, the sensitivity of this method was also affected by the aspecific adsorption of plasma interferents on PS surface. In fact, the slope of the linear fit decreased from 0.017 to 0.0075 upon incubation in plasma.

These preliminary results show a linear response of the sensor in a real sample both in fluorescence and refractive index measurements and prove the good BMP–AA binding selectivity even in presence of several interferents contained in plasma such as proteins, glucose, clotting factors, mineral ions, hormones. The three key concentrations of AA (50, 100 and 200 μM) chosen for the plasma test have been observed in some pathological conditions. In psoriasis, for instance, skin inflamed tissue can contain AA levels of around 100 μM (Hammarstrom et al., 1975). In kidney pathologies AA (50 μM) has been found to constrict isolated perfused renal arteries and potentiate the myogenic response in the presence of indomethacin (Kauser et al., 1991). It has been also demonstrated that AA at micromolar concentrations (around 40 μM) produces a drastic increase in the generation of reactive oxygen species in rat hepatoma AS-30D cells (Dymkowska et al., 2006; Dymkowska and Wojtczak, 2009) along with an increase in the incidence of apoptotic cell death. This has been shown for several types of cell lines cultivated in vitro (Penzo et al., 2002). This sensor could be used as a fast screening method for the AA symptomatic of apoptosis, as an alternative or complementary method to flow cytometry that is the currently used technique to follow apoptosis. The role of AA on liver cancer has been also investigated in rat hepatoma H22 cells and AA concentrations in a range of 7–250 μM have been detected (Xu et al., 2010). In this study the AA was derivatized by p-bromoacetophenone for detection under ultraviolet light by a HPLC system. Our method, instead, would allow a quantification of AA in the same concentration range without any further derivatization procedure.

5. Conclusions

A PS based biosensor for the detection of AA was fabricated. The possibility of using a combination of two different transduction methods based on two different physical mechanisms, one based on fluorescence intensity changes and the second on refractive index changes, on the same sensor was demonstrated, allowing an overlapping comparison of the sensing response.

Interestingly, preliminary results in a real sample, such as blood plasma, showed the linearity of the sensor response for both transduction methods and proved the selectivity of this system even in presence of several interferents. A test representative of three key concentrations measured in some important disease has been carried out with success.

Studies have shown that the concentrations of extracellular, unbound, and free AA in a physiological setting range from the nanomolar (nM) to the micromolar (μM) (Brash, 2001; Omole et al., 2009). The method described in this work instead has a detection range for AA in micromolar concentrations. Our aim for the future

is to increase the dynamic range of the sensor reaching a sensitivity at the nanomolar range.

This detection method could be applied to other P450 enzymes as well as other proteins where the binding of a ligand causes a conformational change.

Acknowledgements

Part of this work was carried out by NanoFacility Piemonte, INRiM, a laboratory supported by Compagnia di San Paolo (Italy).

V.E.V. Ferrero, S.J. Sadeghi and G. Gilardi acknowledge support from the PRIN-MIUR 2006 (Nos. 2006028219 and 2006027587) and from the CIPE 2006 Regione Piemonte (IT).

References

Brash, A.R., 2001. J. Clin. Invest. 107 (11), 1339–1345.
Canham, L., 1997. Properties of Porous Silicon. INSPEC, London.
Chan, S., Horner, S.R., Fauchet, P.M., Miller, B.L., 2001a. J. Am. Chem. Soc. 123 (47), 11797–11798.
Chan, S., Li, Y., Rothberg, L.J., Miller, B.L., Fauchet, P.M., 2001b. Mater. Sci. Eng. C 15 (1–2), 277–282.
Cunin, F., Milhiet, P.E., Anglin, E., Sailor, M.J., Espenel, C., Le Grimellec, C., Brunel, D., Devoisselle, J.M., 2007. Ultramicroscopy 107 (10–11), 1048–1052.
Dai, D., Zeldin, D.C., Blaisdell, J.A., Chanas, B., Coulter, S.J., Ghanayem, B.I., Goldstein, J.A., 2001. Pharmacogenetics 11 (7), 597–607.
Darios, F., Davletov, B., 2006. Nature 440 (7085), 813–817.
Davison, B.H., Nghiem, N.P., 1999. Abstr. Paper. Am. Chem. Soc. Natl. Meet., p. 217, 032-Fuel.
De Lorimier, R.M., Smith, J.J., Dwyer, M.A., Looger, L.L., Sali, K.M., Paavola, C.D., Rizk, S.S., Sadigov, S., Conrad, D.W., Loew, L., Hellinga, H.W., 2002. Protein Sci. 11 (11), 2655–2675.
De Stefano, L., Rendina, N., Moretti, L., Tundo, S., Rossi, A.M., 2004. Appl. Opt. 43 (1), 167–172.
DeLouise, L.A., Miller, B.L., 2005. Anal. Chem. 77 (7), 1950–1956.
Der, B.S., Dattelbaum, J.D., 2008. Anal. Chem. 375 (1), 132–140.
Dymkowska, D., Szczepanowska, J., Wieckowski, M.R., Wojtczak, L., 2006. Biochim. Biophys. Acta 1763 (2), 152–163.
Dymkowska, D., Wojtczak, L., 2009. Acta Biochim. Pol. 56 (4), 711–715.
Fantuzzi, A., Capri, E., Mak, L.H., Dodhia, V.R., Sadeghi, S., Huq, E., Collins, S., Somers, G., Gilardi, G., 2010. Anal. Chem. 82, 10222–10227.
Ferrero, V.E.V., Andolfi, L., Di Nardo, G., Sadeghi, S.J., Fantuzzi, A., Cannistraro, S., Gilardi, G., 2008. Anal. Chem. 80 (22), 8438–8446.
Ferrero, V.E.V., Di Nardo, G., Catucci, G., Sadeghi, S.J., Gilardi, G., 2011. Dalton T., submitted for publication.
Foll, H., 1991. Appl. Phys. A: Mater. Sci. Process. 53 (1), 8–19.
Gilardi, G., Zhou, L.Q., Hibbert, L., Cass, A.E.G., 1994. Anal. Chem. 66 (21), 3840–3847.
Hain, R.D.W., 1997. Palliative Med. 11 (5), 341–350.
Haines, D.C., Tomchick, D.R., Machius, M., Peterson, J.A., 2001. Biochemistry 40 (45), 13456–13465.
Hammarstrom, S., Hamberg, M., Samuelsson, B., Duell, E.A., Stawiski, M., Voorhees, J.J., 1975. Proc. Natl. Acad. Sci. U. S. A. 72 (12), 5130–5134.
Kauser, K., Clark, J.E., Masters, B.S., Demontellano, P.R.O., Ma, Y.H., Harder, D.R., Roman, R.J., 1991. Circ. Res. 68 (4), 1154–1163.
Li, H., Darwish, K., Poulos, L.T., 1991. J. Biol. Chem. 266 (18), 11909–11914.
Ligler, F.S., Taitt, C.R., Shriver-Lake, L.C., Sapsford, K.E., Shubin, Y., Golden, J.P., 2003. Anal. Bioanal. Chem. 377 (3), 469–477.
Lin, V.S.Y., Motesharei, K., Dancil, K.P.S., Sailor, M.J., Ghadiri, M.R., 1997. Science 278 (5339), 840–843.
MacBeath, G., 2001. Nat. Biotechnol. 19 (9), 828–829.
Narhi, L.O., Fulco, A.J., 1986. J. Biol. Chem. 261, 7160–7169.
Nguyen, X., Wang, M.H., Reddy, K.M., Falck, J.R., Schwartzman, M.L., 1999. Am. J. Physiol. 276 (6), R1691–R1700.
Omole, M.A., Noah, N., Zhou, L., Almaletti, A., Sadik, O.A., Asemota, H.N., William, E.S., Gilchrist, J., 2009. Anal. Biochem. 395 (1), 54–60.
Omura, T., Sato, R., 1964. J. Biol. Chem. 239, 2370–2385.
Pacholski, C., Yu, C., Miskelly, G.M., Godin, D., Sailor, M.J., 2006. J. Am. Chem. Soc. 128 (13), 4250–4252.
Panico, P., Dodhia, V.K., Fantuzzi, A., Gilardi, G., 2011. Anal. Chem. 83, 2179–2186.
Panigrahy, D., Kaipainen, A., Greene, E.R., Huang, S., 2010. Cancer Metast. Rev. 29 (4), 723–735.
Penzo, D., Tagliapietra, C., Colonna, R., Petronilli, V., Bernardi, P., 2002. Biochim. Biophys. Acta Bioenerg. 1555 (1–3), 160–165.
Peterson, J.A., Graham, S.E., 1998. Struct. Fold. Des. 6 (9), 1079–1085.
Renard, M., Bedouelle, H., 2004. Biochemistry 43 (49), 15453–15462.
Roman, R.J., 2002. Physiol. Rev. 82 (1), 131–185.
Rong, G., Najmaie, A., Sipe, J.E., Weiss, S.M., 2008. Biosens. Bioelectron. 23 (10), 1572–1576.
Rossi, A.M., Wang, L., Reipa, V., Murphy, T.E., 2007. Biosens. Bioelectron. 23 (5), 741–745.
Sadeghi, S., Fantuzzi, A., Gilardi, G., 2011. Biochim. Biophys. Acta 1814, 237–248.
Sanchez-Mejia, R.O., Mucke, L., 2010. Biochim. Biophys. Acta 1801 (8, Special Issue).
Serhan, C.N., Gotlinger, K., Hong, S., Arita, M., 2004. Prostaglandins Other Lipid Mediators 73 (3–4), 155–172.
Snow, P.A., Squire, E.K., Russell, P.S.J., Canham, L.T., 1999. J. Appl. Phys. 86 (4), 1781–1784.
Su, P., Kaushal, K.M., Kroetz, D.L., 1998. Am. J. Physiol. 275 (2), 426–438.
Vrancken, K.C., Possemiers, K., Vandervoort, P., Vansant, E.F., 1995. Colloids Surf. A 98 (3), 235–241.
Wang, J., 2006. Biosens. Bioelectron. 21 (10), 1887–1892.
Wyss-Coray, T., Mucke, L., 2002. Neuron 35 (3), 419–432.
Xu, Z.G., Zhang, M., Lv, X.Y., Xiang, D., Zhang, X., Chen, L., 2010. Biochem. Cell Biol. 88 (4), 603–609.
Zeldin, D.C., Moomaw, C.R., Jesse, N., Tomer, K.B., Beetham, J., Hammock, B.D., Wu, S., 1996. Arch. Biochem. Biophys. 330 (1), 87–96.